Tuning the magnetic properties of $LaCoO_3$ thin films by epitaxial strain

D. Fuchs,[1] E. Arac,[1,2] C. Pinta,[1,2] S. Schuppler,[1] R. Schneider,[1] and H. v. Löhneysen[1,2]
[1]*Forschungszentrum Karlsruhe, Institut für Festkörperphysik, 76021 Karlsruhe, Germany*
[2]*Physikalisches Institut, Universität Karlsruhe, 76128 Karlsruhe, Germany*
(Received 18 October 2007; published 24 January 2008)

Ferromagnetic order can be induced in $LaCoO_3$ (LCO) thin films by epitaxial strain. Here, we show that the magnetic properties can be "tuned" by epitaxial strain imposed on LCO thin films by the epitaxial growth on various substrate materials, i.e., (001) oriented $SrLaAlO_4$, $LaAlO_3$, $SrLaGaO_4$, $(LaAlO_3)_{0.3}(Sr_2AlTaO_6)_{0.7}$, and $SrTiO_3$. The lattice mismatch at room temperature of the in-plane lattice parameters between the substrate, a_s, and bulk LCO, a_b, ranges from −1.31% to +2.63%. Single-phase, ⟨001⟩ oriented LCO thin films were grown by pulsed laser deposition on all these substrates. Due to the difference of the thermal-expansion coefficients between LCO and the substrates, the films experience an additional tensile strain of about +0.3% during the cooling process after the deposition at $T_s=650$ °C. The film lattice parameters display an elastic behavior, i.e., an increase of the in-plane film lattice parameter with increasing a_s. From the ratio between the out-of-plane and in-plane strain, we obtain a Poisson ratio of $\nu \approx 1/3$. All films show a ferromagnetic transition as determined from magnetization measurements. The magnetization increases strongly with increasing tensile strain, whereas the transition temperature T_C after a rapid initial rise appears to saturate at $T_C \approx 85$ K above $a=3.86$ Å. The effective magnetic moment μ_{eff} in the paramagnetic state increases almost linearly as a function of the mean lattice parameter $\langle a \rangle$, indicating an enhanced population of higher spin states, i.e., intermediate- or high-spin states. The experimental results are discussed in terms of a decrease of the octahedral-site rotation with increasing tensile strain.

DOI: 10.1103/PhysRevB.77.014434 PACS number(s): 75.70.−i, 75.70.Ak, 75.30.Et

I. INTRODUCTION

Among the rare-earth transition metal oxides with perovskite structure, the lanthanum cobaltate $LaCoO_3$ (LCO) exhibits unusual electronic and magnetic properties at ambient pressure.[1,2] At low temperature, $T \leqslant 35$ K, LCO is a nonmagnetic semiconductor with a ground state of Co^{3+} ions of a low spin (LS) configuration ($t_{2g}^6 e_g^0$, $S=0$).[3] This is believed to change to a primarily intermediate-spin (IS) ($t_{2g}^5 e_g^1$, $S=1$) state[4] in the temperature range $35\ \text{K} < T < 100$ K and further to a mixture of IS and high-spin (HS) ($t_{2g}^4 e_g^2$, $S=2$) states in the interval $300\ \text{K} < T < 600$ K. The existence of IS has been questioned recently on the basis of x-ray absorption spectroscopy and magnetic circular dichroism.[5] The crossover between spin states with increasing temperature arises from a delicate interplay between the crystal-field splitting Δ_{CF}, i.e., the splitting between the t_{2g} and e_g energy levels, and the intra-atomic exchange interaction (Hund's rule coupling) Δ_{ex}. The balance between Δ_{CF} and Δ_{ex} can be influenced by, e.g., hole or electron doping,[6] and by chemical or external pressure.[7] The crystal-field splitting is very sensitive to changes of the interatomic distances r since $\Delta_{\text{CF}} \propto r^{-5}$.[8] Therefore, the spin states of LCO strongly depend on variations of the Co-O bond length d and the Co-O-Co bonding angle β. An increase of d leads, for example, to a decrease of Δ_{CF} and can thus cause an increased population of higher spin states.

Very recently, we have demonstrated that the population of higher spin states, i.e., IS and HS states, is significantly enhanced in strained LCO films epitaxially grown on $(LaAlO_3)_{0.3}(Sr_2AlTaO_6)_{0.7}$ (LSAT) substrates.[9] In contrast to the nonmagnetic LS ground state of bulk LCO, we observed ferromagnetic order below $T_C \approx 85$ K. It is likely that the epitaxial strain leads to a suppression of the Jahn-Teller distortion (JTD), which may be regarded as a prerequisite for a ferromagnetic superexchange interaction. Solovyev *et al.* investigated by local-spin-density-approximation calculations how lattice defects affect the magnetic behavior in $LaMnO_3$ (Mn^{3+}: $t_{2g}^3 e_g^1$). They demonstrated that the absence of the JTD leads to a positive e_g-type exchange between occupied and unoccupied orbitals, which prevails over the negative t_{2g}-type exchange, resulting in an FM ground state of $LaMnO_3$.[10] A suppression of the JTD in LCO has, indeed, been observed very recently by infrared spectroscopy on ferromagnetic LCO nanoparticles.[11]

The high sensitivity of the magnetization of LCO to strain motivates the present work where we have investigated the influence of epitaxial strain on the magnetic properties of LCO in more detail. In order to "tune" the strain, we have deposited LCO films epitaxially on single-crystal substrates with different in-plane lattice parameters that are expected to influence the epitaxial strain and thus the bond lengths and bond angles of the LCO film provided that an elastic coupling between film and substrate material exists. In addition to the prerequisites for epitaxial growth such as chemical stability and lattice matching, a good matching of the thermal-expansion coefficients between the film and substrate material is required. Because of the pseudocubic crystal structure of perovskites, the substrate material should have a square-shaped surface cell allowing for a "cube-on-cube growth" of the LCO films, i.e., the in-plane a axis and b axis of the film are oriented parallel to the a and b axes of the substrate material, respectively. The following commercially available substrate materials are suitable for the film deposition: (001) oriented $SrLaAlO_4$ (SLAO), $LaAlO_3$ (LAO), $SrLaGaO_4$ (SLGO), $(LaAlO_3)_{0.3}(Sr_2AlTaO_6)_{0.7}$

TABLE I. In-plane lattice parameters of the used substrate materials, a_s, and the corresponding lattice mismatch, $\varepsilon=(a_s-a_b)/a_b$, to $LaCoO_3$ at room temperature. a_b corresponds to the pseudocubic bulk lattice parameter of $LaCoO_3$. The mismatch at the deposition temperature $T_s=650$ °C is denoted by ε^*.

Substrate	Orientation	Abbreviation	a_s (Å)	ε (%)	ε^* (%)
$SrLaAlO_4$	(001)	SLAO	3.75	−1.31	−2.46
$LaAlO_3$	(001)	LAO	3.78	−0.52	−1.68
$SrLaGaO_4$	(001)	SLGO	3.84	+1.05	−0.12
$(LaAlO_3)_{0.3}$ $(Sr_2AlTaO_6)_{0.7}$	(001)	LSAT	3.87	+1.84	+0.67
$SrTiO_3$	(001)	STO	3.90	+2.63	+1.44

(LSAT), and $SrTiO_3$ (STO). In the following, we report on the structural and magnetic properties of LCO films grown epitaxially on these substrates.

II. EXPERIMENT

For the preparation of strained LCO films, we used ⟨001⟩ oriented SLAO, LAO, SLGO, LSAT, and STO substrates. The room-temperature in-plane lattice parameters a_s of the substrates and the corresponding lattice mismatch to LCO, $\varepsilon=(a_s-a_b)/a_b$, where $a_b=3.80$ Å corresponds to the pseudocubic lattice parameter of bulk LCO, are listed in Table I. The lattice mismatch ranges from $\varepsilon=-1.31\%$ for LCO films on SLAO ($a_s<a_b$) to $\varepsilon=+2.63\%$ for films on STO ($a_s>a_b$). Since the film deposition is carried out at $T_s=650$ °C, well above room temperature, we also list the mismatch ε^* at T_s. The corresponding lattice parameters a_s at T_s were calculated using a thermal-expansion coefficient of $\alpha_S \approx 1\times10^{-5}/\mathrm{K}$.[12] For LCO, we used $a_b=3.869$ Å at T_s.[13,14] Due to the larger thermal-expansion coefficient of LCO, i.e., $\alpha_{\mathrm{LCO}}\approx 2\times10^{-5}/\mathrm{K}$,[13] the lattice mismatch at T_s deviates significantly from that at room temperature. The difference of the thermal-expansion coefficients ($\alpha_{\mathrm{LCO}}-\alpha_S>0$) leads to an additional tensile stress in the film with decreasing temperature.

The film deposition was carried out by pulsed laser deposition using an excimer laser with $\lambda=248$ nm and stoichiometric sinter targets of LCO. The films were deposited with a film thickness of about 100 nm. The deposition parameters such as substrate temperature and oxygen partial pressure were chosen to obtain the highest crystalline quality of the films. The fluence and repetition rate of the laser pulses as well as the target-substrate distance were adopted from a previous optimization of the LCO growth on LSAT.[9] After deposition, the samples were cooled down at a rate of about 10 K/min to 500 °C, where they were kept for 30 min in 0.9 bar oxygen atmosphere to ensure a complete and homogeneous oxygenation of the films, and finally were cooled down with 10 K/min to room temperature.

For the characterization of the structural properties of the epitaxial films such as the out-of-plane c-axis lattice parameter and the mosaic spread, we carried out $\theta/2\theta$ scans and rocking curves on a two-circle x-ray diffractometer. Reciprocal-space mapping on asymmetric Bragg reflections on a four-circle x-ray diffractometer equipped with Cu $K\alpha$ radiation was used to characterize the in-plane lattice parameters a and b and the epitaxial strain. The composition of the films was checked by Rutherford backscattering spectrometry and energy dispersive x-ray analysis.

The magnetic properties of the films were studied using a Quantum Design MPMS superconducting quantum interference device system. The field-cooled (FC) magnetization was measured in the temperature range $4\ \mathrm{K}\leqslant T\leqslant 150$ K. The external field with a strength of $\mu_0 H=20$ mT was applied parallel to the film surface. The diamagnetic contribution of the substrate was determined in separate runs and subtracted from the magnetization data.

The macroscopic magnetization reversal processes were observed with magneto-optical Kerr effect (MOKE) vector magnetometry in polar and longitudinal configurations. Measurements of the magnetization components in both directions allow a precise determination of the orientation of the hard and easy axes.

III. RESULTS AND DISCUSSION

A. Structural properties

Single-phase ⟨001⟩ oriented LCO films were grown successfully on all substrate materials. All films showed a "cube-on-cube" growth on the single-crystal substrates. The quality of the epitaxial growth was characterized by the mosaic spread of the films determined from the full width at half maximum of the rocking curves at the (002) film reflection. The mosaic spread for films grown on SLAO, LAO, and STO was comparable and amounts to about 0.15°. However, films grown on SLGO and LSAT showed always a slightly smaller mosaic spread of about 0.1°. The excellent growth of LCO films on SLGO and LSAT is most likely favored by the small lattice mismatch at T_s compared to the other substrates.

The out-of-plane lattice parameter c was deduced from $\theta/2\theta$ scans on (00l) reflections. The in-plane lattice parameters a and b were determined from asymmetric Bragg reflections which we scanned with a four-circle x-ray diffractometer. In Fig. 1, we show the lattice parameters and the cube root of the unit-cell volume, $V^{1/3}=(a\times b\times c)^{1/3}$, of the LCO films as a function of the in-plane lattice parameter a_s of the substrate material. As expected for an epitaxially strained film, the in-plane film lattice parameter a increases

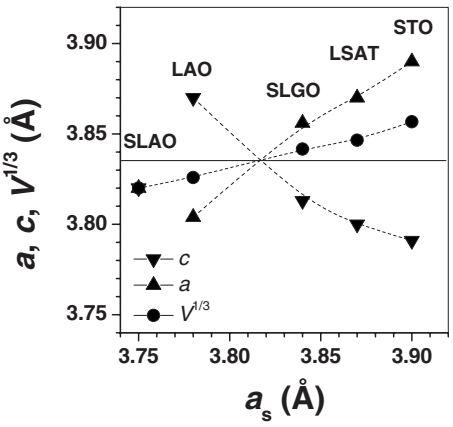

FIG. 1. Lattice parameters a (triangles) and c (inverted triangles) and the cube root of the unit-cell volume $V^{1/3}$ (circles) of the LCO films as a function of the lattice parameter a_s of the corresponding substrate material at room temperature. The dashed lines are guides to the eyes.

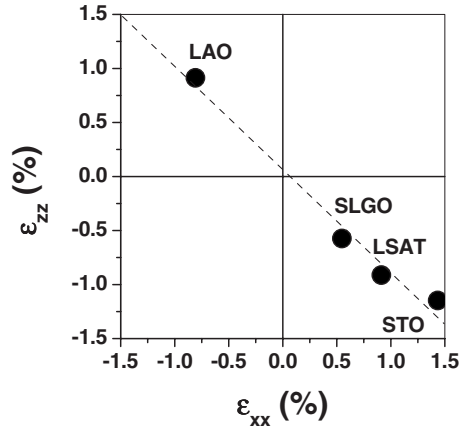

FIG. 2. Out-of-plane lattice strain ε_{zz} versus the in-plane lattice strain ε_{xx}. The dashed line is a linear fit to the data points and reflects $\varepsilon_{zz} \approx -\varepsilon_{xx}$ which results in a Poisson ratio of $\nu = 1/3$.

and the out-of-plane lattice parameter c decreases with increasing a_s, resulting in a pseudotetragonal structure. The tetragonal distortion, $\Delta_{TD} = |a-c|/(a+c)$, is largest for the films on STO and LAO, i.e., 2.6% and 2.3%, respectively, and nearly negligible for the films on SLAO. However, deviations from the nearly linear dependence of a and c on a_s are clearly present for the LCO films grown on SLAO and to some extent for films on STO. These are the samples with the largest negative and positive lattice mismatch ε^*, respectively. On the one hand, films grown on SLAO seem to be strongly relaxed with a pseudocubic structure and lattice parameters of $a=b\approx c=3.82$ Å. Although the LCO films on SLAO seem to be fully relaxed, some residual strain is imposed during the preparation or cooldown, as evidenced by the slightly larger lattice constant compared to bulk LCO. On the other hand, the growth on STO substrates results in a formation of macroscopic cracks in the films after deposition, which can be nicely observed by optical light microscopy. The cracking is most likely caused by a structural relaxation and the relief of tensile strain because of the large lattice mismatch of $\varepsilon = +2.63\%$. Since such a cracking behavior is only observed for LCO films on STO, stress due to the thermal mismatch which is approximately the same for all the substrate-LCO combinations does not seem to be the primary cause of crack formation.

The unit-cell volume V increases by about +3% with increasing a_s, which in turn increases by about +4% for the substrates employed. It is obvious that the pseudocubic lattice parameter for LCO which we determined by $V^{1/3}$ is always larger than the expected room-temperature value of bulk LCO, $a_b=3.80$ Å. The larger unit-cell volume is possibly caused by the difference of the thermal-expansion coefficients between the film, α_{LCO}, and substrate, α_S. Due to the smaller thermal-expansion coefficient of the substrates, the epitaxially "clamped" LCO films are subjected to a tensile load during the cooling process after film deposition. The thermal stress σ_{th} which is exerted on the film can be roughly estimated by $\sigma_{th} = \Delta\alpha \times \Delta T \times E/(1-\nu)$ with $\Delta\alpha$, ΔT, E, and ν being the difference of the thermal-expansion coefficients, the temperature difference, the Young modulus, and the Poisson ratio of LCO, respectively. Assuming $E \approx 150$ GPa (Ref. 15) and $\nu \approx 0.3$ (Ref. 16) for bulk LCO, we obtain for the thermal tensile stress $\sigma_{th} \approx +1.35$ GPa.[17] Since $\alpha_S \approx 0.5\alpha_{LCO}$, the temperature-induced decrease of the lattice constant "experienced" by the LCO film is only half of that for bulk LCO, resulting in structural properties corresponding to those of LCO at $T \approx 335$ °C. The pseudocubic lattice parameter of bulk LCO at that temperature is $V^{1/3} \approx 3.84$ Å,[13] in very good agreement with our results presented in Fig. 1. The data in Fig. 1 suggest that a pseudocubic structure with $a \approx c := a_c = 3.835$ Å is obtained at $a_s \approx 3.815$ Å. The obtained value of $a_c = 3.835$ Å corresponds quite well to that of unstrained bulk LCO at $T \approx 335$ °C. This demonstrates that besides the epitaxial strain arising from the lattice mismatch, the tensile load during the cooling process is playing a crucial role for the structural properties of the epitaxial LCO films.

The elastic properties of the LCO films are shown in more detail in Fig. 2, where we have plotted the out-of-plane lattice strain, $\varepsilon_{zz} = (c-a_c)/a_c$, versus the in-plane lattice strain, $\varepsilon_{xx} = (a-a_c)/a_c$. Here, the lattice strain is defined as the deviation from the pseudocubic lattice parameter $a_c = 3.835$ Å. The data for the strongly relaxed LCO film on SLAO are not displayed in the figure. A linear fit to the data, shown by the dashed line, results in a slope of $\varepsilon_{zz}/\varepsilon_{xx} \approx -1$, yielding the Poisson ratio $\nu = 1/(1-2\times\varepsilon_{xx}/\varepsilon_{zz}) = 1/3$, in good agreement with literature data.[16] $\nu \approx 1/3$ has been observed previously for epitaxially strained films of hole-doped cobaltates, i.e., $La_{0.7}A_{0.3}CoO_3$ (A=Ca, Sr, or Ba),[18] and appears to be typical of the manganites as well.[19] Hence, we can conclude that there is a nearly perfect elastic coupling between the film and substrate.

To characterize the homogeneity of the epitaxial strain, we carried out a reciprocal-space mapping on asymmetric Bragg reflections ($h=k\neq l$) along the [hh0] and [00l] directions. Only the LCO films on LSAT showed a fully strained growth, i.e., $a=a_s$. For the other films of the same thickness $d \approx 100$ nm, we observed a slight difference between a and a_s which might be explained by a partial structural relaxation

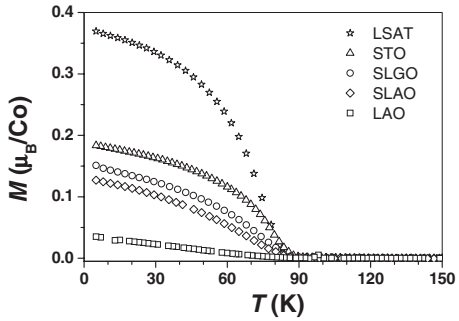

FIG. 3. Field-cooled magnetization of LCO films on various substrate materials. The magnetic field strength of $\mu_0 H = 20$ mT was applied parallel to the film surface.

of the film. On the other hand, measurements on thinner films with $d \approx 50$ nm and films with $d \approx 200$ nm displayed nearly the same lattice parameters, so that the strain in the investigated films with $d \approx 100$ nm can be regarded as more or less homogeneous. This is consistent with our previous observations on hole-doped cobaltates, e.g., $La_{0.7}Sr_{0.3}CoO_3$, where we have found a noticeable structural relaxation only within the first tens of nanometers of film growth.[20] We also carried out scans along the so-called "relaxation line"[21] at Bragg reflections of different orders, e.g., the (112) and (222), or the (113) and (223) reflections. This technique provides some overall information on how strain evolves as a function of film thickness.[22] Because of the lower penetration depth of x rays with decreasing Bragg angle due to absorption, measurements at smaller angles are more sensitive to the surface region. However, within the experimental resolution of our four-circle x-ray diffractometer, we were not able to detect any significant change of the strain with increasing order of the Bragg reflection. From these results, we conclude that the films are strained quite homogeneously.

B. Magnetic properties

In Fig. 3, we display the field-cooled magnetization of the LCO films on the various substrates as a function of temperature in a magnetic field $\mu_0 H = 20$ mT applied parallel to the film surface. In contrast to the nonmagnetic ground state of LCO, the epitaxially strained films clearly exhibit a ferromagnetic (FM) transition. To highlight this observation, we plot in Fig. 4 the inverse susceptibility H/M versus T for the LCO films on the various substrates. The paramagnetic Curie-Weiss temperature Θ, which is obtained by the extrapolation of H/M to zero, is positive and close to the Curie temperature T_C obtained from M versus T. As demonstrated previously, the strain-induced ferromagnetism is not simply a property of the surface region and rather extends over the complete film thickness.[9] Both the magnetization and the FM onset temperature of the LCO films in Fig. 3 decrease systematically with decreasing in-plane film lattice parameter. We emphasize again that for all thin-film systems, the in-plane film lattice parameters and unit-cell volumes as determined from x-ray diffraction measurements were larger than those of bulk LCO.

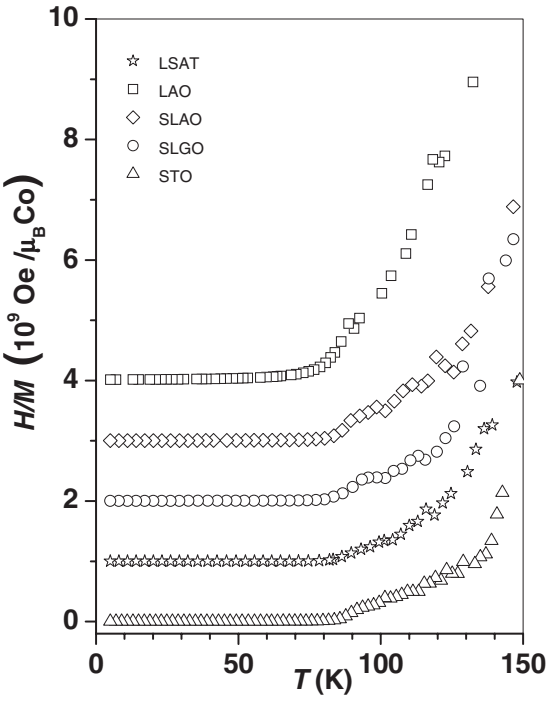

FIG. 4. The inverse of the susceptibility H/M versus T for LCO films on various substrates. Data are offset vertically for clarity.

The magnetization reversal process in the ferromagnetic state was characterized by MOKE vector magnetometry. In order to elucidate a possible magnetic anisotropy in the LCO films, the measurements were carried out in polar and longitudinal configurations. Figure 5 displays in-plane and out-of-plane magnetization reversal loops for LCO on LSAT (top)

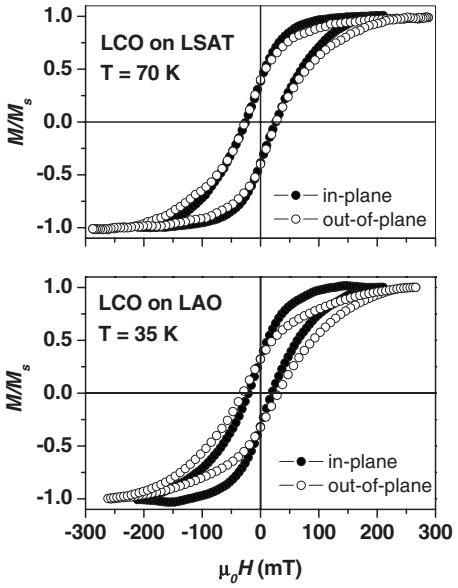

FIG. 5. In-plane and out-of-plane magnetization reversal loops normalized to the saturated magnetization M_s for LCO films on LSAT (top) and LAO (bottom) at $T/T_C \approx 0.8$. For the in-plane (out-of-plane) magnetization, the field was applied parallel (perpendicular) to the film surface.

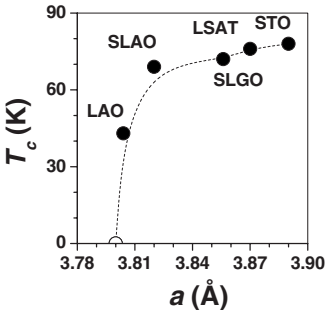

FIG. 6. The Curie temperature T_C as a function of the in-plane film lattice parameter a. The data points are labeled with the corresponding substrates. The data point for bulk LCO is denoted by the circle. Dashed line is a guide to the eyes.

and on LAO (bottom) at $T/T_C \approx 0.8$. The similar coercive field and remnant magnetization values as well as the shapes of polar and longitudinal loops indicate the absence of a distinct anisotropy.

Figure 6 shows the Curie temperature T_C as a function of the in-plane film lattice parameter a. T_C was determined from the minimum of the derivative of the FC magnetization, dM/dT. It is obvious that T_C increases very rapidly with increasing lattice constant a and seems to saturate around 85 K above $a=3.86$ Å. A possible explanation for this trend could be an increase of the Co-O-Co bonding angle β toward 180° with increasing a. An increase of β toward 180° leads to a stronger hybridization of the Co $3d$ and O $2p$ orbitals and thus very likely to an increased bandwidth or even overlap of the e_g-derived bands. According to the Goodenough-Kanamori-Anderson rules[23,24] and to our scenario described in Ref. 9, this favors the ferromagnetic superexchange between occupied and unoccupied e_g orbitals, where the exchange interaction should increase with increasing hybridization, i.e., β.

In bulk LCO, the alternating octahedral-site rotation leads to $\beta \approx 163°$, resulting in a strong rhombohedral distortion of the crystal structure.[13] The rotation of the oxygen octahedra is correlated with the unit-cell volume and the A-site ion radius. It is strongly reduced or even absent if the A sites of the ABO_3 perovskite structure are substituted by larger ions. For instance, Sr doping of LCO ($La_{1-x}Sr_xCoO_3$) leads to an increase of the unit-cell volume and, for $x \geq 0.55$,[25] to a rhombohedral-cubic structural phase transition with a complete "untilting" of the oxygen octahedra, i.e., $\beta \approx 180°$. If the Co-O bond length d does not change, an increase of the in-plane lattice parameters results in a reduced Co-O-Co tilt angle (larger β). From Co K-edge x-ray absorption measurements on LCO films on LSAT at $T=15$ K, we were able to determine a single value Co-O bond length of $d=1.92$ Å within an accuracy of $\pm 2\%$.[26] A distinct splitting of the bond lengths, i.e., into a short and a long Co-O bond, which may be expected by the tetragonal distortion of the unit-cell could not be observed. Hence, a tetragonal distortion of the oxygen octahedra which would lead to a splitting of the e_g orbitals appears to be absent. Usually, the JTD leads to two different Co-O bond lengths which at room temperature differ by about 6% in bulk LCO[27] and by even 10% for $LaMnO_3$.[28] Thus, the JTD is strongly reduced or even absent in the epitaxial LCO films.

d of our epitaxial films is identical to the value of bulk LCO (at $T \approx 15$ K) (Ref. 29) and therefore is apparently not affected by the tensile strain and it is only β that changes toward 180°. This is also verified by the second-shell Co-O-Co-like paths, from x-ray absorption measurements, amounting for the LCO film on LSAT to 3.85 Å which is nearly twice the value of d. For bulk LCO, the room-temperature value of d is 1.93 Å.[29] Since the measured in-plane film lattice parameter of LCO on LSAT, $a=3.87$ Å, is only slightly larger than $2d$, β should be fairly close to 180°. Of course, a further increase of β is not possible, and this may explain why T_C saturates above $a=3.86$ Å.

In contrast to the increase of the FM coupling within the ab plane with increasing a, the coupling along the c axis may not be ferromagnetic because of the decreasing lattice parameter c. For the LCO films with $c \leqslant 3.82$ Å, a bonding angle of $\beta \leqslant 166°$ along the c axis is expected if a constant Co-O bond length of 1.93 Å is assumed. Because of the rather large deviation from $\beta=180°$, the coupling along the two Co-O bonds of the oxygen octahedra along the c axis might be antiferromagnetic (AFM). However, in contrast to $LaMnO_3$ where the exchange between the ab planes (along the c axis) is AFM due to the rather strong exchange of the t_{2g}^3 HS ($S=3/2$) states, the AFM exchange between the t_{2g} orbitals in LCO might be reduced because of the smaller t_{2g} spin moment of the Co^{3+} IS (t_{2g}^5, $S=1/2$) and HS (t_{2g}^4, $S=1$) states. We note that an antiferro-orbital ordering might also lead to FM coupling.[23]

In the following, we will give a qualitative account of the evolution of the effective moment μ_{eff} with tensile strain, while we cannot at present explain the rapid initial increase of T_C in Fig. 6 which of course is affected by the "generation" of magnetic moments with the increase of tensile strain. Previous results obtained on LCO films on LSAT have shown that tensile strain can stabilize or even enhance the population of IS and HS states.[9] In comparison with the effective magnetic moment of bulk LCO of $\mu_{\text{eff}}=1.96\ \mu_B/\text{Co}$ in the temperature range of $100\ \text{K} < T < 300\ \text{K}$,[29,30] epitaxially strained LCO films on LSAT show a considerably higher effective moment of $\mu_{\text{eff}}=3.87\ \mu_B/\text{Co}$. In order to investigate the influence of epitaxial strain on the paramagnetic state, we have determined μ_{eff} from the susceptibility between 100 and 150 K, yielding effective magnetic moments ranging from 2.8 μ_B/Co for LCO on SLAO up to 4.6 μ_B/Co for LCO on STO.

The increase of the magnetic moment can be attributed by an increased population of higher spin states. In a single-ion picture where $\mu_{\text{eff}}=g_e\sqrt{S(S+1)}$, with the electron g factor $g_e \approx 2$, μ_{eff} depends very sensitively on the spin state of the Co ions. The increased population of IS and HS states is primarily due to a reduction of the energy difference ΔE between the crystal-field splitting and the intra-atomic exchange interaction (Hund's rule coupling), i.e., $\Delta E(\Delta_{\text{CF}} - \Delta_{\text{ex}})$, which leads to a redistribution of electrons between the t_{2g} and e_g levels. In a simple crystal-field picture for nondistorted oxygen octahedra, the LS state is stable if Δ_{CF} is larger than the on-site Coulomb repulsion, whereas the HS

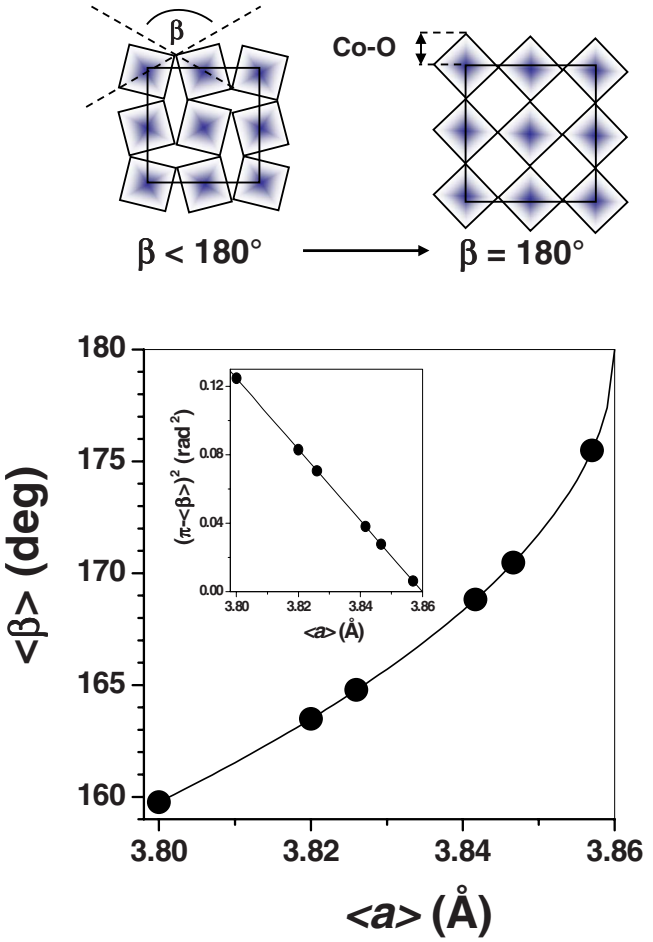

FIG. 7. (Color online) The mean Co-O-Co bond angle $\langle\beta\rangle$ calculated from the mean lattice parameter $\langle a\rangle=(2/3a+1/3c)=2d\cos[(\pi-\langle\beta\rangle)/2]$ as a function of $\langle a\rangle$. The inset shows $(\pi-\langle\beta\rangle)^2$ versus $\langle a\rangle$. The solid line is a linear fit to the data points and demonstrates the validity of the first order Taylor series approximation. The sketch above the diagram shows the untilting of the oxygen octahedra with increasing β if the Co-O bond length d is kept constant. Note that with increasing β, the unit-cell volume increases.

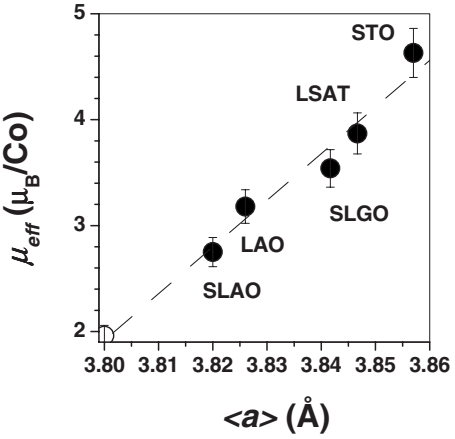

FIG. 8. The effective paramagnetic moment μ_{eff} of LCO films as a function of the mean lattice parameter $\langle a\rangle=(2/3a+1/3c)$ (closed symbols). The data points are labeled with the names of the corresponding substrates. The bulk value of LCO is displayed by the open symbol. The dashed line is a linear fit to the data points.

state dominates for larger Δ_{ex}. The IS state can be stabilized by a distortion of the octahedra, e.g., by a Jahn-Teller effect which splits the e_g levels and thereby reduces the energy difference ΔE. Furthermore, a strong hybridization between Co e_g orbitals and p orbitals of the oxygen ligands favors the IS state, as has been shown by calculations based on density-functional theory.[4,29] The hybridization broadens the bandwidth W of the d-p bands, which reduces the energy difference to[7] $([\Delta_{\text{CF}}-W/2]-\Delta_{\text{ex}})$, and makes the t_{2g} and e_g bands overlap. Since the bandwidth is given by[31] $W\propto\cos(\pi-\beta)/d^{3.5}$, higher spin states are not only stabilized by a decrease of Δ_{CF} but also by an increase of W, i.e., an increase of the Co-O-Co bond angle β and a decrease of the Co-O bond length d. However, since Δ_{CF} changes with d^{-5} in the point-charge approximation,[8] the IS state is more stable than the LS state for structures with longer Co-O distances and larger Co-O-Co bond angles. For a constant distance d, the increase of μ_{eff} should therefore scale with the increase of $\cos(\pi-\beta)$. For small angles $(\pi-\beta)$, $\cos(\pi-\beta)\approx 1-(\pi-\beta)^2/2$, yielding a linear dependence of μ_{eff} on $(\pi-\beta)^2$.

In a simple structural picture, the lattice parameter a can be expressed in terms of the Co-O bond distance and the Co-O-Co bond angle by $a=2d\cos[(\pi-\beta)/2]$, which leads in view of the above considerations to a linear dependence of a on $(\pi-\beta)^2$ and thus to a linear dependence of μ_{eff} on a. From the above formula, β can be calculated if a and d are known. In order to take into account the tetragonal distortion of the unit cell of the epitaxially strained LCO films and hence different Co-O-Co bond angles along the [100]/[010] and [001] axes, we have used an averaged lattice parameter $\langle a\rangle=(2/3a+1/3c)$. Using $d=1.93$ Å, the mean Co-O-Co bond angle $\langle\beta\rangle$ is shown in Fig. 7 as a function of $\langle a\rangle$. The inset shows $(\pi-\langle\beta\rangle)^2$ versus $\langle a\rangle$. The solid line is a linear fit to the data, which demonstrates the validity of the simple approach. The sketch above the diagram shows the "untilting" of the oxygen octahedra with increasing β for a constant Co-O bond length, d.

Finally, Fig. 8 shows μ_{eff} as a function of the mean lattice parameter $\langle a\rangle$. The dashed line is a linear fit to the data points and reflects very well the linear dependence of μ_{eff} on a expected from the simple model. Assuming a single-ion picture and a simple spin model consisting only of LS and HS (IS and HS) states, the evolution of the measured μ_{eff} with increasing tensile strain can be interpreted as an increase of the occupation of the HS state starting from 30% ($\approx$0%) for bulk LCO to 75% (50%) for LCO films on LSAT up to about 92% (85%) for LCO films on STO. This rough estimate demonstrates the strong impact of epitaxial strain on the magnetic properties of LCO films. Another explanation for the increase of μ_{eff} with the increase of tensile strain would be an increased contribution of the orbital moment. In order to investigate this in more detail, x-ray absorption spectroscopy and soft x-ray magnetic circular dichroism measurements on strained LCO films are planned.

IV. CONCLUSIONS

Epitaxially strained thin films of LCO have been prepared by pulsed laser deposition on different substrate materials. Because of the square-shaped surface unit cell of the chosen substrate materials, the films could be grown in a cube-on-cube growth mode. The lattice mismatch of the in-plane lattice parameters between the substrate, a_s, and LCO, a_b, ranges from $\varepsilon=-1.31\%$ to $+2.63\%$. The nearly linear behavior of a and c with the substrate lattice parameter a_s within the range of $-1\% < \varepsilon < 2\%$ indicates an elastic coupling of the film to the substrate and therefore the possibility to tune the epitaxial strain in a specific way. Due to the difference of the thermal-expansion coefficients of the substrate and film, $\Delta\alpha$, the LCO films experience an additional thermally induced stress which results in a larger pseudocubic lattice parameter of $a_c=3.835$ Å in comparison with that of bulk LCO. From the ratio of the in-plane and out-of-plane strain, $\varepsilon_{zz}/\varepsilon_{xx}=-1$, we obtain a Poisson ratio of $\nu=0.3$.

For all the epitaxial LCO films, we observed a FM transition below 85 K. The transition temperature T_C and the magnetization increase strongly with increasing in-plane film lattice parameter a, i.e., tensile strain, where T_C seems to saturate at $T_C \approx 85$ K above $a=3.86$ Å. The effective magnetic moment μ_{eff} in the paramagnetic state increases nearly linearly as a function of the mean lattice parameter $\langle a \rangle$ which may indicate an enhanced population of IS or HS spin states. Since the Co-O bond length d was found to be not affected by the tensile strain and compares well to that of bulk LCO, the results can be explained by the decrease of the octahedral-site rotation with increasing tensile strain. The increase of the mean Co-O-Co bonding angle $\langle \beta \rangle$ toward 180° leads to an increased hybridization of the Co $3d-$O $2p$ orbitals. An additional hybridization of the e_g-derived bands may be provided by a suppression of the Jahn-Teller splitting of the e_g levels due to the "clamping" effect of the epitaxy. This favors a ferromagnetic superexchange interaction and the population of higher spin states which, in conjunction with a possible antiferro-orbital ordering, is very likely the reason for the observed FM state in epitaxially strained LCO films. Further work will be necessary to check if strain tuning provides a road toward quantum criticality in this system.

ACKNOWLEDGMENT

Part of this work was partly supported by the DFG in the frame of the Research Unit *Forschungsgruppe 960* Quantum Phase Transitions.

[1] G. H. Jonker, J. Appl. Phys. **37**, 1424 (1966).
[2] P. M. Raccah and J. B. Goodenough, Phys. Rev. **155**, 932 (1967).
[3] J. Q. Yan, J. S. Zhou, and J. B. Goodenough, Phys. Rev. B **69**, 134409 (2004).
[4] M. A. Korotin, S. Y. Ezhov, I. V. Solovyev, V. I. Anisimov, D. I. Khomskii, and G. A. Sawatzky, Phys. Rev. B **54**, 5309 (1996).
[5] M. W. Haverkort, Z. Hu, J. C. Cezar, T. Burnus, H. Hartmann, M. Reuther, C. Zobel, T. Lorenz, A. Tanaka, N. B. Brookes, H. H. Hsieh, H. J. Lin, C. T. Chen, and L. H. Tjeng, Phys. Rev. Lett. **97**, 176405 (2006).
[6] D. Fuchs, P. Schweiss, P. Adelmann, T. Schwarz, and R. Schneider, Phys. Rev. B **72**, 014466 (2005).
[7] J. S. Zhou, J. Q. Yan, and J. B. Goodenough, Phys. Rev. B **71**, 220103(R) (2005).
[8] D. M. Sherman, in *Advances in Physical Geochemistry*, edited by S. K. Saxena (Springer, Berlin, 1988).
[9] D. Fuchs, C. Pinta, T. Schwarz, P. Schweiss, P. Nagel, S. Schuppler, R. Schneider, M. Merz, G. Roth, and H. v. Löhneysen, Phys. Rev. B **75**, 144402 (2007).
[10] I. Solovyev, N. Hamada, and K. Terakura, Phys. Rev. Lett. **76**, 4825 (1996).
[11] S. M. Zhou, L. Shi, J. Y. Zhao, L. F. He, H. P. Yang, and S. M. Zhang, Phys. Rev. B **76**, 172407 (2007).
[12] The thermal-expansion coefficient is nearly the same for all the used substrate materials and amounts to approximately $\alpha \approx 1 \times 10^{-5}/\text{K}$. See also M. Drozdowski, J. Domagala, M. Kozielski, M. Szybowicz, and A. Pajaczkowska, Solid State Commun. **96**, 785 (1995) for SLGO; P. Byszewski, J. Domagala, J. Finkfinowicki, and A. Pajaczkowska, Mater. Res. Bull. **27**, 483 (1992) for SLAO; M. Berovski, J. Fink. Finowicki, R. Diduszko, P. Byszewski, R. Aleksiyko, and R. Kikalejshvili-Domukhovska, J. Cryst. Growth **257**, 146 (2003) for LSAT; D. de Ligny and P. Richet, Phys. Rev. B **53**, 3013 (1996) for STO.
[13] P. G. Radaelli and S. W. Cheong, Phys. Rev. B **66**, 094408 (2002).
[14] V. Ramaswamy, P. Awati, and A. K. Tyagi, J. Alloys Compd. **364**, 180 (2004).
[15] T. Vogt, J. A. Hriljac, N. C. Hyatt, and P. Woodward, Phys. Rev. B **67**, 140401(R) (2003).
[16] N. Orlovskaya, K. Kleveland, T. Grande, and M. A. Einarsrud, J. Eur. Ceram. Soc. **20**, 51 (2000).
[17] In comparison with the stress which can be achieved by the use of a conventional anvil cell, the stress obtained by epitaxial growth due to the mismatch of the thermal-expansion coefficients between the film and substrate material can be much higher. For that reason, epitaxial growth provides the possibility to realize large stress.
[18] For the hole-doped cobaltates, $La_{0.7}A_{0.3}CoO_3$ with A=Ca, Sr, or Ba, we were able to deposit compressive strained films on $LaAlO_3$ with $\varepsilon_{xx} \approx -0.5\%$, -1%, and -2%, respectively.
[19] G. Fehringer, S. Janes, M. Wildersohn, and R. Clasen, J. Eur. Ceram. Soc. **24**, 705 (2004).
[20] D. Fuchs, T. Schwarz, O. Moran, P. Schweiss, and R. Schneider, Phys. Rev. B **71**, 092406 (2005).
[21] The relaxation line is the line in the reciprocal space which connects the positions of the reciprocal lattice points of the fully strained, i.e., $a=a_s$, and the fully relaxed state, i.e., $a=a_b$.
[22] V. Holy, U. Pietsch, and T. Baumbach, *High resolution x-ray scattering from thin films and multilayers*, Springer tracts in modern physics (Springer, Berlin, 1999).
[23] D. I. Khomskii and G. A. Sawatzky, Solid State Commun. **102**, 87 (1997).

[24] T. Mizokawa and A. Fujimori, Phys. Rev. B **51**, 12880 (1995).
[25] A. Mieshige, M. Inaba, T. Yao, Z. Ogumi, K. Kokutchi, and M. Kawase, J. Solid State Chem. **121**, 423 (1996).
[26] C. Pinta, D. Fuchs, E. Pellegrin, P. Adelmann, S. Mangold, and S. Schuppler, J. Low Temp. Phys. **147**, 421 (2007).
[27] G. Maris, Y. Ren, V. Volotchaev, C. Zobel, T. Lorenz, and T. T. M. Palstra, Phys. Rev. B **67**, 224423 (2003).
[28] J. Rodriguez-Carvajal, M. Hennion, F. Moussa, A. H. Moudden, L. Pinsard, and A. Revcolevschi, Phys. Rev. B **57**, R3189 (1998).
[29] K. Kniaek, P. Novak, and Z. Jirak, Phys. Rev. B **71**, 054420 (2005).
[30] D. P. Kozlenko, N. O. Golosova, Z. Jirak, L. S. Dubrovinsky, B. N. Savenko, M. G. Tucker, Y. LeGodec, and V. P. Glazkov, Phys. Rev. B **75**, 064422 (2007).
[31] W. A. Harrison, *The Electronic Structure and Properties of Solids* (Freeman, San Francisco, 1980).